Research Article

NMR IN BIOMEDICINE

Received: 20 April 2010, Revised: 14 July 2010, Accepted: 14 July 2010, Published online in Wiley Online Library: 3 October 2010

(wileyonlinelibrary.com) DOI:10.1002/nbm.1604

In vivo mapping of tumor oxygen consumption using ^{19}F MRI relaxometry

Caroline Diepart[a], Julie Magat[a], Bénédicte F. Jordan[a]† and Bernard Gallez[a]*†

Recently, we have developed a new electron paramagnetic resonance (EPR) protocol in order to estimate tissue oxygen consumption *in vivo*. Because it is crucial to probe the heterogeneity of response in tumors, the aim of this study was to apply our protocol, together with ^{19}F MRI relaxometry, to the mapping of the oxygen consumption in tumors. The protocol includes the continuous measurement of tumor pO_2 during the following respiratory challenge: (i) basal values during air breathing; (ii) increasing pO_2 values during carbogen breathing until saturation of tissue with oxygen; (iii) switching back to air breathing. We have demonstrated previously using EPR oximetry that the kinetics of return to the basal value after oxygen saturation are mainly governed by tissue oxygen consumption. This challenge was applied in hyperthyroid mice (generated by chronic treatment with L-thyroxine) and control mice, as hyperthyroidism is known to dramatically affect the oxygen consumption rate of tumor cells. Our recently developed snapshot inversion recovery MRI fluorocarbon oximetry technique allowed the pO_2 return kinetics to be measured with a high temporal resolution. The kinetic constants (i.e. oxygen consumption rates) were higher for tumors from hyperthyroid mice than from control mice, data that are consistent with our previous EPR study. The corresponding histograms of the ^{19}F MRI data showed that the kinetic constants displayed a shift to the right for the hyperthyroid group, indicating a higher oxygen consumption in these tumors. The color maps showed a large heterogeneity in terms of oxygen consumption rate within a tumor. In conclusion, ^{19}F MRI relaxometry allows the noninvasive mapping of the oxygen consumption in tumors. The ability to assess the heterogeneity of tumor response is critical in order to identify potential tumor regions that might be resistant to treatment and therefore produce a poor response to therapy. Copyright © 2010 John Wiley & Sons, Ltd.

Keywords: tumor oxygenation; oxygen consumption; ^{19}F MRI; tumor microenvironment

INTRODUCTION

Hypoxia plays a crucial role in the resistance of tumors to chemo- and radiotherapy. Several studies have shown improved outcomes for cancer patients whose tumors have lower hypoxic fractions (1). Tumor hypoxia depends on the balance between oxygen supply and consumption, and both factors should be considered when developing strategies to reduce tumor hypoxia. A number of strategies have been considered in an effort to improve tumor oxygenation during radiation treatment, with the goal of increasing tumor sensitivity to irradiation. The theoretical simulation of oxygen handling in tumors (2) suggests that decreasing the oxygen consumption rate of tumor tissue could be a particularly effective strategy to reduce the fraction of hypoxic tissue in solid tumors. Indeed, several pharmacological drugs that inhibit cellular oxygen consumption have been characterized *in vivo* for their potential to increase tumor oxygenation, and thereby to enhance radiosensitivity. *meta*-Iodobenzylguanidine (3), insulin (4–6), anti-inflammatory drugs (7), corticoids (8), inhibitors of vascular endothelial growth factor receptor tyrosine kinase (SU5416 and ZD6474) (9,10) and thyroid hormones (11) all play a major role in the metabolism of tumor cells by modifying the rate of oxygen consumption. Other means of reducing oxygen consumption have been proposed, including the administration of glucose, via the Crabtree effect (12) and decreasing local tumor temperature to less than 25°C (13).

Given the importance of oxygen, many techniques for measuring pO_2 in living animals and humans have been developed (14), but methods to measure rates of oxygen consumption *in vivo* are more limited. Among these methods, positron emission tomography allows the *in vivo* measurement and quantification of physiological processes using short-lived positron-emitting radiopharmaceuticals. This technique enables the measurement of cerebral oxygen consumption using a short inhalation of [^{15}O]-O_2 (15,16). However, this method cannot be applied in tissues with disorganized vascular architecture, such as tumors. The quantitative blood oxygenation level-dependent technique is MRI based and provides a regional *in vivo* oxygen extraction fraction measurement of brain, defining oxygen consumption (17,18). However, this technique provides only an

* *Correspondence to: B. Gallez, REMA, Avenue Mounier 73.40, B-1200 Brussels, Belgium.*

a *C. Diepart, J. Magat, B. F. Jordan, B. Gallez*
Biomedical Magnetic Resonance Group, Louvain Drug Research Institute, Université Catholique de Louvain, Brussels, Belgium

† *B. F. Jordan and B. Gallez are co-senior authors.*

Abbreviations used: *EPR, electron paramagnetic resonance; HFB, hexafluorobenzene; ROI, region of interest; S/N, signal-to-noise ratio; SNAP-IR, snapshot inversion recovery.*

indirect measurement of oxygen consumption as the method is based on a theoretical model and the deoxyhemoglobin content can be affected by both the local blood flow and volume. ^{17}O MRI has also been used to measure cerebral blood flow and oxygen consumption in the cat brain. This technique has the potential to image cerebral blood flow and oxygen consumption in humans, but does not provide a direct measurement of oxygen consumption (19,20). Moreover, this technique requires flow measurements. Dewhirst *et al.* (21) reported determinations of the oxygen consumption rate in microscopic tumor regions bound by microvessels using oxygen microelectrodes. Theoretical simulations of oxygen diffusion in the regions were made, and consumption rates were estimated for the best fit between measured and simulated values. However, such electrodes are difficult to use, involve a significant degree of invasiveness and cannot be employed for repeated measurements. Near-infrared spectroscopy can provide an approach to quantify tumor oxygen consumption rate by a mathematical model, but the method requires animal sacrifice. The model describes changes in tumor oxyhemoglobin concentration as a function of time before and after potassium chloride-induced cardiac arrest (22).

Recently, we have developed a new *in vivo* electron paramagnetic resonance (EPR) oximetry protocol that can estimate tissue oxygen consumption noninvasively (23). For this purpose, we designed a protocol in which pO_2 was monitored in the tissue of interest during a breathing challenge: (i) basal values during air breathing; (ii) increasing pO_2 values during carbogen breathing until saturation of tissue with oxygen; (iii) rapidly decreasing pO_2 values when switching back to air breathing. We thereby showed that the kinetics of the return to the basal value after oxygen saturation were mainly governed by tissue oxygen consumption. To validate our approach, we applied this protocol in muscle and tumor tissues in hyperthyroid and control mice. Hyperthyroidism is known to dramatically affect the oxygen consumption rate of muscle and tumor cells (11,24). It was induced by chronic treatment with L-thyroxine. Muscle and tumor cells from hyperthyroid mice consumed oxygen faster than muscle and tumor cells from control mice, data that were consistent with *in vitro* studies (11). Tumor perfusion was not affected by treatment with L-thyroxine. We qualified this method as being able to give an index of local oxygen consumption. Although the measure is indirect, it provides the unique advantage of being adapted to *in vivo* studies (23).

In this study, we applied the breathing challenge protocol to map the oxygen consumption of tumors using ^{19}F MR relaxometry after intratumoral injection of hexafluorobenzene (HFB) (25). This spatial information is critical to probe the heterogeneous aspect of the oxygen consumption in tumors. ^{19}F MRI has been developed by Mason and coworkers (26–29) to image pO_2, as well as to follow dynamic changes in tumors. Our group recently adapted this method using snapshot inversion recovery (SNAP-IR) in order to increase the time resolution with a similar spatial resolution (30). The technique was applied to monitor acute changes in pO_2 in an experimental tumor model. Here, we demonstrate the feasibility of monitoring *in vivo* tumor oxygen consumption using a SNAP-IR ^{19}F MRI protocol.

MATERIALS AND METHODS

Tumor model

A transplantable mouse liver tumor model was implanted in the gastrocnemius muscle of NMRI mice. The measurements were performed when the tumor reached 8.0 ± 1.0 mm (1 week after tumor cell injection). Tumors were implanted in hyperthyroid and control mice ($n = 6$ for each group). Hyperthyroid mice were obtained by treating mice with L-thyroxine (0.003%) in drinking water for 3 weeks prior to tumor transplantation. All animal experiments were conducted in accordance with national animal care regulations.

Animal preparation

Before MRI measurements, animals were anesthetized by inhalation of isoflurane mixed with 21% oxygen in a continuous flow, delivered by a nose cone. Induction of anesthesia was performed using 3% of isoflurane, and then isoflurane was stabilized at 1.8% for a minimum of 15 min before any measurement. Isoflurane was chosen as it does not compromise tumor hemodynamics (31).

HFB was deoxygenated by bubbling nitrogen for 5 min before use. It was injected into the tumor and deposited along three tracks (3×30 μL) encompassing both central and peripheral regions. Warm air was used during MRI acquisition to maintain mouse body temperature.

^{19}F MRI measurements

MRI was performed with a 4.7-T (200-MHz, ^{1}H) bore system (inner diameter, 40 cm) (Bruker Biospec, Ettlingen, Germany). A tunable ^{1}H/^{19}F surface coil was used for radiofrequency transmission and reception. MRI scout images were obtained for both ^{1}H (200.1 MHz) and ^{19}F (188.3 MHz). HFB parametric images of the spin–lattice relaxation time (T_1) were estimated using a SNAP-IR pulse sequence (30). The pulse sequence consisted of a nonselective hyperbolic, secant inversion pulse, followed by acquisition of a series of 512 rapid gradient echo images (TR = 10.9 ms; TE = 4.2 ms; flip angle, 1°; matrix, 32×16; field of view, 60×30 mm^2; bandwidth, 12.5 kHz; total acquisition time, 1.5 min). Raw (*k*-space) data were zero-filled to a matrix size of 64×64, resulting in interpolated 64×64 images.

The measurement of oxygen consumption was performed using a protocol described previously (23). When three identical measurements had been obtained under air breathing conditions, the breathing gas was switched to carbogen. Carbogen breathing was maintained until the local pO_2 reached a maximum (45 min according to EPR) (23). The gas was then switched back to air, and measurements were made until pO_2 returned to its basal value. Measurements were performed at 10-min intervals during the first part of the experiment (before switching back to air), and at 3-min intervals during the second part of the experiment.

Data processing

Data were processed using home-built routines in Matlab (The MathWorks Inc., Natick, MA, USA).

^{19}F MRI analysis

For each ^{19}F MR image, a polygonal region of interest (ROI) encompassing the tumor was defined. For each voxel, the signal-to-noise ratio (S/N) was estimated and voxels with S/N < 5 were removed. A nonlinear fit was used to determine the T_1 relaxation in each pixel of the ROI (a three-parameter fit was performed on the signal intensity during the inversion time using the standard inversion recovery equation), having a T_1 error/T_1

ratio of less than 50%. A time–T_1 map was created with $0 < T_1 < 10$ ms according to Eqn (1).

The calibration curve between the relaxation rate R_1 ($R_1 = 1/T_1$) and pO_2 was estimated in previous work on *in vitro* samples (30):

$$pO_2(mmHg) = \frac{R_1(s^{-1}) - 0.1048}{0.002} \quad (1)$$

The correlation between T_1 (s) and pO_2 (mmHg) was used to obtain a map of the partial oxygen pressure for each voxel. We estimated that pO_2 values had to be less than 500 mmHg. Even though the evolution of pO_2 was observed during the entire breathing protocol, only the p_{o2} values after switching back to air breathing were considered for further analysis, as the return kinetics have been shown to be related to oxygen consumption [see 'Introduction' and ref. (23)]. The return kinetics were estimated by a monoexponential fit [$a\ \exp(-kx) + b$], where the k value represents the kinetics of oxygen consumption (min^{-1}). Fitting conditions were as follows: relative difference between two consecutive pO_2 values of less than 5% and each voxel with a k value between zero and unity.

k-map analysis

A map of pO_2 return kinetics in each voxel was obtained, showing both experimental and fitted data. Data were normalized and voxels with a mean relative error between experimental and fitted data of greater than 30% were not considered. Finally, aberrant voxels corresponding to fitting with less than five points were removed.

RESULTS AND DISCUSSION

Typical changes in tumor pO_2 assessed using ^{19}F MR relaxometry during the breathing challenge are shown in Fig. 1. The first arrow corresponds to the start of the carbogen challenge. The second arrow corresponds to the time at which carbogen was switched back to air. The sampling time of our SNAP-IR technique allowed the return kinetics to be probed with a sufficient temporal resolution. Quantitative estimation of the return kinetics was carried out using a monoexponential curve, as this estimation fitted well with the experimental data (Fig. 1) (23). As shown previously with EPR oximetry, the thyroid status modified significantly the kinetic constants. The kinetic constants of tumors from hyperthyroid mice were higher than those of control tumors (Fig. 2A). The k values were $0.076 \pm 0.01\ min^{-1}$ (mean $\pm$ standard error, $n = 6$) and $0.125 \pm 0.015\ min^{-1}$ (mean $\pm$ standard error, $n = 6$) in control and treated tumors, respectively; each k value was assessed from an ROI encompassing the whole tumor, and k values were then averaged between groups and compared statistically (Student's t-test, $p < 0.05$). The corresponding histogram (reflecting averaged k values from both groups) was also generated, showing a shift of the kinetic constants to the right (lower k values) for the treated tumors (i.e. from hyperthyroid mice) (Fig. 2B). The results obtained by ^{19}F MRI were similar to those from our previous EPR study: a significant difference between tumors from control and hyperthyroid mice was observed and the typical changes in pO_2 also matched well with the EPR technique (similar patterns were observed in response to carbogen breathing with both techniques). However, the range of absolute k values did not match between the two techniques. This further emphasizes the fact that our method does not provide a quantitative absolute value of oxygen consumption, but rather an index that may reasonably be ascribed to the local oxygen consumption. This difference in terms of k values can be explained by the intrinsic differences in the two techniques for probing oxygenation: EPR spectroscopy provides local measurements (mean sampling volume of 10 mm^3) that can

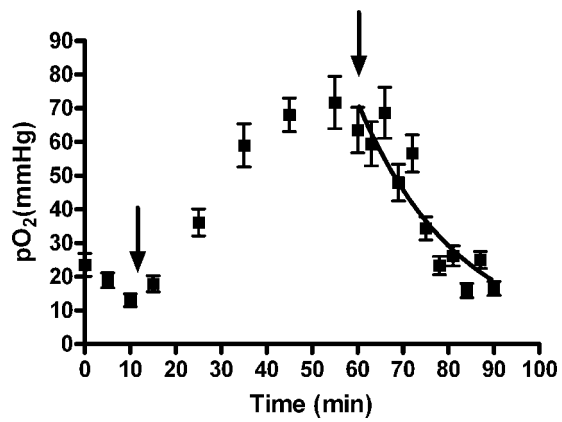

Figure 1. Typical changes in pO_2 (mmHg) over time (min) during the breathing challenge in one control tumor. First arrow: air switched to carbogen; second arrow: carbogen switched to air.

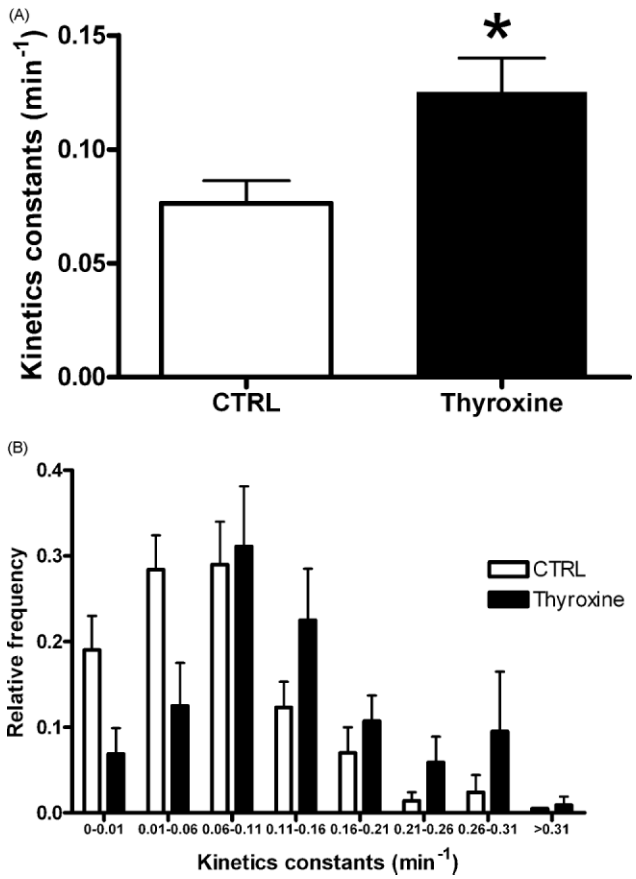

Figure 2. (A) Mean kinetic constants (min^{-1}) measured in tumors for control (CTRL) and thyroxine treatment. The kinetic constants measured in tumors from hyperthyroid mice were higher than those in control mice (averaged on all tumors). $^*p < 0.05$. (B) Corresponding cumulative normalized histogram of different k values obtained using ^{19}F MRI data for all mice, generated by defining regions of interest encompassing the whole tumor.

be greatly influenced by highly hypoxic regions (32), whereas ^{19}F MR relaxometry provides parametric oxygen values (quantitative mapping of oxygenation) that are usually higher than those found using other techniques (including invasive fiber-optic probes), as observed by our group and others (25,30,33), probably because of the lipophilic property of the sensor (HFB) in which oxygen is more soluble. Although some earlier reports have argued that HFB localizes to chronically hypoxic regions and shows values in good agreement with electrode-derived pO_2 (34), we believe that we interrogated both poorly perfused (chronically hypoxic) regions and well-perfused regions according to the distribution of the basal pO_2 values, as well as the large response observed during carbogen breathing, as further discussed in our first HFB study (30). Nevertheless, the *k* (consumption rates) values can be qualified as qualitative parameters that can be compared between treatments using a single technique, but cannot be compared from one technique to another.

We have shown previously that perfusion is not responsible for the change in return kinetics, and that local oxygen consumption is the main factor responsible for this return to initial oxygenation levels. Indeed, a clamping experiment confirmed that our technique measured the oxygen consumption of tumor cells without any major influence of confounding factors, such as perfusion and vascular pO_2 (23). However, in the future, it would be interesting to measure perfusion by a dynamic contrast-enhanced MRI study to completely rule out any influence on the kinetic constants, and to develop a combined method with appropriate analysis in order to exclude any confounding factors of perfusion. In addition, no correlation was found between tumor pO_2 at saturation (maximal pO_2 during the carbogen challenge) or baseline pO_2 values

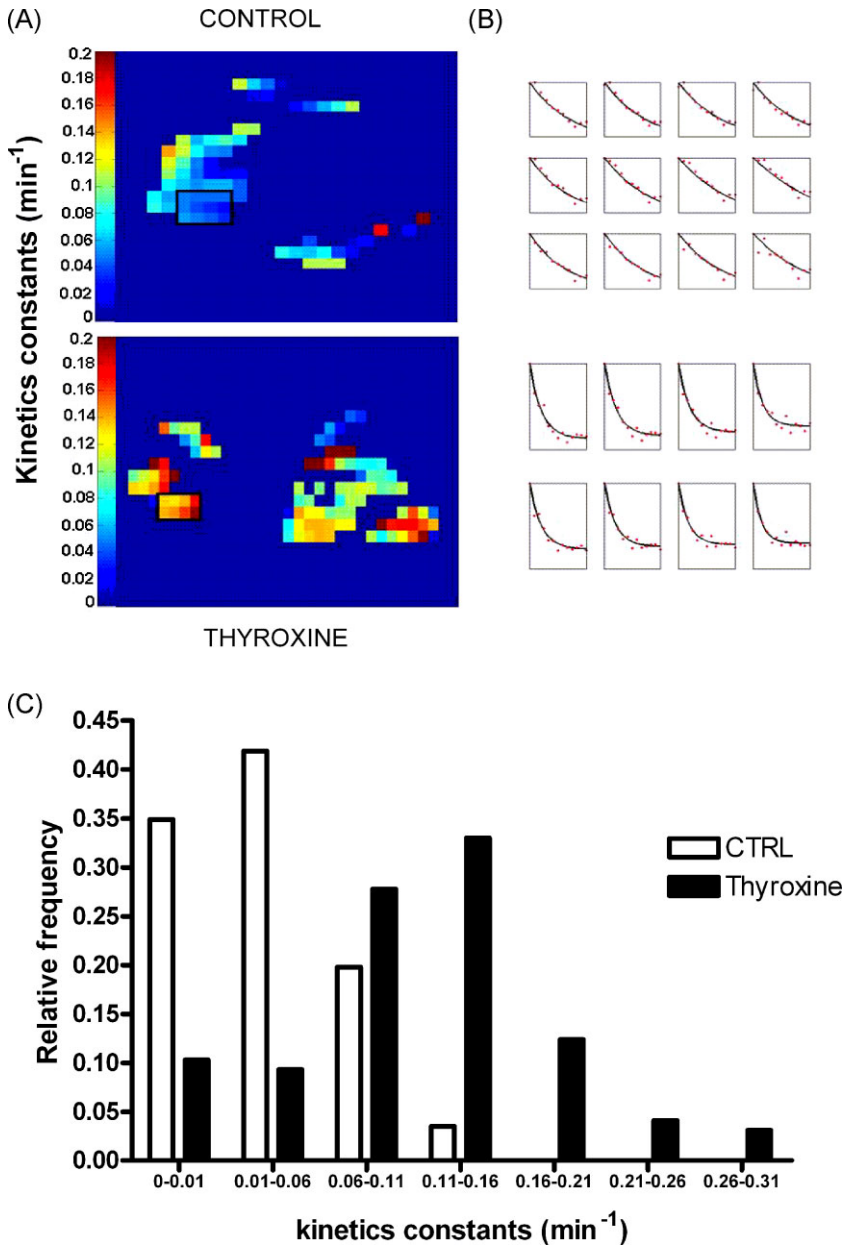

Figure 3. (A) Typical oxygen consumption map (min^{-1}) overlaid on an anatomical ^{1}H MR image of one control and one hyperthyroid tumor after carbogen challenge. (B) Evolution of kinetic constants for the selected pixels: full line, fitted data; red points, experimental data. (C) Typical cumulative normalized histogram of *k* values of the corresponding control (CTRL) and hyperthyroid tumors (generated pixel by pixel from a single tumor).

and kinetic constants; therefore, these factors do not influence the estimation of the oxygen consumption rate (data not shown). Moreover, constants were determined on normalized graphs (see below, Fig. 3B).

For each tumor, we generated color kinetic constant maps derived from the ^{19}F MRI data in each pixel of the tumor, reflecting the heterogeneity in *k* values caused by differences in oxygen consumption. Figure 3A shows typical oxygen consumption maps for a control tumor and for a tumor implanted in a hyperthyroid mouse. A difference in the kinetic constants between control and treated tumors can be seen, marked by a global increase in the red color (corresponding to high kinetic constants) (Fig. 3A). The pO_2 evolution of each pixel in an arbitrary ROI is illustrated in Fig. 3B (initial pO_2 is normalized to unity in each pixel). We can see that the return to baseline for control mice takes much longer than for treated mice. A typical histogram of the corresponding typical tumors, representing all *k* values from all the pixels within the tumor, was also generated (Fig. 3C). It shows a clear shift to the right of the kinetic constants of the tumors in treated mice (i.e. tumors from hyperthyroid mice). This analysis therefore includes the spatial intratumoral heterogeneity information (Fig. 3), contrary to the analysis showing the averaged histograms generated from ROIs encompassing the whole tumor (Fig. 2).

CONCLUSION

^{19}F MR relaxometry was successfully used to provide maps of an oxygen consumption index in experimental tumors (constants extracted from the return kinetics after an hyperoxic challenge, an index that may be reasonably ascribed to the local oxygen consumption). We found considerable intratumoral heterogeneity in the distribution of the kinetic constants. Indeed, in spite of a difference in oxygen consumption between control and hyperthyroid mice, both showed a large variability in terms of *k* values. Oxygen consumption by tumor cells might therefore be responsible for intratumoral pO_2 heterogeneity, together with the chaotic architecture of the vascular network. This technique offers the unique advantage of being able to probe oxygen consumption *in vivo* in a noninvasive manner, together with the generation of spatial information that is required to probe heterogeneity. The ability to assess the heterogeneity of tumor response is critical in order to identify potential tumor regions that might be resistant to treatment and lead to a poor response to therapy. Currently, no clinical application of perfluorocarbon oximetry has been carried out because of the invasiveness and biocompatibility issues of the intratumoral implantation of perfluorocarbons (33).

Acknowledgements

This work was supported by grants from the Belgian National Fund for Scientific Research (FNRS), the Televie, the Fonds Joseph Maisin, the Saint-Luc Foundation, the Actions de Recherches Concertées-Communauté Française de Belgique-ARC 09/14-020 and the Pôle d'attraction Interuniversitaire PAI VI (P6/38). BJ is a research associate of the FNRS.

REFERENCES

1. Vaupel P, Harrison L. Tumor hypoxia: causative factors, compensatory mechanisms, and cellular response. Oncologist, 2004; 9(Suppl 5): 4–9.
2. Secomb TW, Hsu R, Ong ET, Gross JF, Dewhirst MW. Analysis of the effects of oxygen supply and demand on hypoxic fraction in tumors. Acta Oncol. 1995; 34: 313–316.
3. Biaglow JE, Manevich Y, Leeper D, Chance B, Dewhirst MW, Jenkins WT, Tuttle SW, Wroblewski K, Glickson JD, Stevens C, Evans SM. MIBG inhibits respiration: potential for radio- and hyperthermic sensitization. Int. J. Radiat. Oncol. Biol. Phys. 1998; 42: 871–876.
4. Jordan BF, Gregoire V, Demeure RJ, Sonveaux P, Feron O, O'Hara J, Vanhulle VP, Delzenne N, Gallez B. Insulin increases the sensitivity of tumors to irradiation: involvement of an increase in tumor oxygenation mediated by a nitric oxide-dependent decrease of the tumor cells oxygen consumption. Cancer Res. 2002; 62: 3555–3561.
5. Jordan BF, Sonveaux P, Feron O, Gregoire V, Beghein N, Dessy C, Gallez B. Nitric oxide as a radiosensitizer: evidence for an intrinsic role in addition to its effect on oxygen delivery and consumption. Int. J. Cancer, 2004; 109: 768–773.
6. Jordan BF, Beghein N, Crokart N, Baudelet C, Gregoire V, Gallez B. Preclinical safety and antitumor efficacy of insulin combined with irradiation. Radiother. Oncol. 2006; 81: 112–117.
7. Crokart N, Radermacher K, Jordan BF, Baudelet C, Cron GO, Gregoire V, Beghein N, Bouzin C, Feron O, Gallez B. Tumor radiosensitization by antiinflammatory drugs: evidence for a new mechanism involving the oxygen effect. Cancer Res. 2005; 65: 7911–7916.
8. Crokart N, Jordan BF, Baudelet C, Cron GO, Hotton J, Radermacher K, Gregoire V, Beghein N, Martinive P, Bouzin C, Feron O, Gallez B. Glucocorticoids modulate tumor radiation response through a decrease in tumor oxygen consumption. Clin. Cancer Res. 2007; 13: 630–635.
9. Ansiaux R, Baudelet C, Jordan BF, Crokart N, Martinive P, Dewever J, Gregoire V, Feron O, Gallez B. Mechanism of reoxygenation after antiangiogenic therapy using SU5416 and its importance for guiding combined antitumor therapy. Cancer Res. 2006; 66: 9698–9704.
10. Ansiaux R, Dewever J, Gregoire V, Feron O, Jordan BF, Gallez B. Decrease in tumor cell oxygen consumption after treatment with vandetanib (ZACTIMA; ZD6474) and its effect on response to radiotherapy. Radiat. Res. 2009; 172: 584–591.
11. Jordan BF, Christian N, Crokart N, Gregoire V, Feron O, Gallez B. Thyroid status is a key modulator of tumor oxygenation: implication for radiation therapy. Radiat. Res. 2007; 168: 428–432.
12. Snyder SA, Lanzen JL, Braun RD, Rosner G, Secomb TW, Biaglow J, Brizel DM, Dewhirst MW. Simultaneous administration of glucose and hyperoxic gas achieves greater improvement in tumor oxygenation than hyperoxic gas alone. Int. J. Radiat. Oncol. Biol. Phys. 2001; 51: 494–506.
13. Kelleher DK, Nauth C, Thews O, Krueger W, Vaupel P. Localized hypothermia: impact on oxygenation, microregional perfusion, metabolic and bioenergetic status of subcutaneous rat tumours. Br. J. Cancer, 1998; 78: 56–61.
14. Tatum JL, Kelloff GJ, Gillies RJ, Arbeit JM, Brown JM, Chao KS, Chapman JD, Eckelman WC, Fyles AW, Giaccia AJ, Hill RP, Koch CJ, Krishna MC, Krohn KA, Lewis JS, Mason RP, Melillo G, Padhani AR, Powis G, Rajendran JG, Reba R, Robinson SP, Semenza GL, Swartz HM, Vaupel P, Yang D, Croft B, Hoffman J, Liu G, Stone H, Sullivan D. Hypoxia: importance in tumor biology, noninvasive measurement by imaging, and value of its measurement in the management of cancer therapy. Int. J. Radiat. Biol. 2006; 82: 699–757.
15. Mintun MA, Raichle ME, Martin WR, Herscovitch P. Brain oxygen utilization measured with O-15 radiotracers and positron emission tomography. J. Nucl. Med. 1984; 25: 177–187.
16. Okazawa H, Kudo T. Clinical impact of hemodynamic parameter measurement for cerebrovascular disease using positron emission tomography and (15)O-labeled tracers. Ann. Nucl. Med. 2009; 23: 217–227.
17. He X, Yablonskiy DA. Quantitative BOLD: mapping of human cerebral deoxygenated blood volume and oxygen extraction fraction: default state. Magn. Reson. Med. 2007; 57: 115–126.
18. He X, Zhu M, Yablonskiy DA. Validation of oxygen extraction fraction measurement by qBOLD technique. Magn. Reson. Med. 2008; 60: 882–888.
19. Pekar J, Ligeti L, Ruttner Z, Lyon RC, Sinnwell TM, van GP, Fiat D, Moonen CT, McLaughlin AC. In vivo measurement of cerebral oxygen consumption and blood flow using ^{17}O magnetic resonance imaging. Magn. Reson. Med. 1991; 21: 313–319.

20. Zhu XH, Zhang N, Zhang Y, Zhang X, Ugurbil K, Chen W. In vivo ^{17}O NMR approaches for brain study at high field. NMR Biomed. 2005; 18: 83–103.
21. Dewhirst MW, Secomb TW, Ong ET, Hsu R, Gross JF. Determination of local oxygen consumption rates in tumors. Cancer Res. 1994; 54: 3333–3336.
22. Song Y, Kim JG, Mason RP, Liu H. Investigation of rat breast tumor oxygen consumption by near-infrared spectroscopy. J. Phys. D: Appl. Phys. 2005; 38: 2682–2690.
23. Diepart C, Jordan BF, Gallez B. A new EPR oximetry protocol to estimate the tissue oxygen consumption in vivo. Radiat. Res. 2009; 172: 220–225.
24. Gredilla R, Lopez TM, Portero-Otin M, Pamplona R, Barja G. Influence of hyper- and hypothyroidism on lipid peroxidation, unsaturation of phospholipids, glutathione system and oxidative damage to nuclear and mitochondrial DNA in mice skeletal muscle. Mol. Cell. Biochem. 2001; 221: 41–48.
25. Zhao D, Jiang L, Mason RP. Measuring changes in tumor oxygenation. Methods Enzymol. 2004; 386: 378–418.
26. Hunjan S, Zhao D, Constantinescu A, Hahn EW, Antich PP, Mason RP. Tumor oximetry: demonstration of an enhanced dynamic mapping procedure using fluorine-19 echo planar magnetic resonance imaging in the Dunning prostate R3327-AT1 rat tumor. Int. J. Radiat. Oncol. Biol. Phys. 2001; 49: 1097–1108.
27. Zhao D, Jiang L, Hahn EW, Mason RP. Tumor physiologic response to combretastatin A4 phosphate assessed by MRI. Int. J. Radiat. Oncol. Biol. Phys. 2005; 62: 872–880.
28. Xia M, Kodibagkar V, Liu H, Mason RP. Tumour oxygen dynamics measured simultaneously by near-infrared spectroscopy and ^{19}F magnetic resonance imaging in rats. Phys. Med. Biol. 2006; 51: 45–60.
29. Mason RP, Rodbumrung W, Antich PP. Hexafluorobenzene: a sensitive ^{19}F NMR indicator of tumor oxygenation. NMR Biomed. 1996; 9: 125–134.
30. Jordan BF, Cron GO, Gallez B. Rapid monitoring of oxygenation by ^{19}F magnetic resonance imaging: simultaneous comparison with fluorescence quenching. Magn. Reson. Med. 2009; 61: 634–638.
31. Baudelet C, Gallez B. Effect of anesthesia on the signal intensity in tumors using BOLD-MRI: comparison with flow measurements by Laser Doppler flowmetry and oxygen measurements by luminescence-based probes. Magn. Reson. Imaging, 2004; 22: 905–912.
32. Gallez B, Baudelet C, Jordan BF. Assessment of tumor oxygenation by electron paramagnetic resonance: principles and applications. NMR Biomed. 2004; 17: 240–262.
33. Robinson SP, Griffiths JR. Current issues in the utility of ^{19}F nuclear magnetic resonance methodologies for the assessment of tumour hypoxia. Philos. Trans. R. Soc. Lond. B. Biol. Sci. 2004; 359: 987–996.
34. McIntyre DJO, McCoy CL, Griffiths JR. Tumour oxygenation measurements by ^{19}F MRI of perfluorocarbons. Curr. Sci. 1999; 76: 753–762.